Proceedings of the
47th IEEE Conference on Decision and Control
Cancun, Mexico, Dec. 9-11, 2008

Close Target Reconnaissance Using Autonomous UAV Formations

Iman Shames, Barış Fidan and Brian D. O. Anderson

Abstract— **In this paper the problem of close target reconnaissance by a formation of 3 unmanned aerial vehicles (UAVs) is considered. The overall close target reconnaissance (CTR) involves subtasks of avoiding obstacles or no-fly-zones, avoiding inter-agent collisions, reaching a close vicinity of a specified target position, and forming an equilateral triangular formation around the target. The UAVs performing the task fly at constant speeds. A decentralized control scheme is developed for this overall task considering unidirectional sensing/control architecture. Relevant analysis and simulation test results are provided.**

I. Introduction

Control and coordination of formations of autonomous agents find many real life civil and defence applications in recent years. The multi-agent autonomous formations can consist of unmanned ground vehicles (UGVs), autonomous underwater vehicles (AUVs), unmanned aerial vehicles (UAVs) or sometimes a combination of more than one agent type. For the special case of formations of UAVs according to [1], a formation of UAVs needs to perform three basic tasks: *(i)* not to let the aircraft hit the ground; *(ii)* not to fly the aircraft beyond their limits; and, *(iii)* not to let each aircraft collide with the others. Furthermore, another task that is as important as the mentioned tasks is not to let each aircraft hit an obstacle during its motion. When these tasks are fulfilled the group of UAVs can accomplish its higher level task [2]. For certain tasks, e.g. identification or precise geolocation of a target, the formation may have to spend some time in the proximity of the target location. This task can be accomplished by moving around the target on a desired circle for fixed-wing UAVs flying with the same constant speed. Along this line of research, [3] and [4] have proposed a control framework under cyclic pursuit, causing the agents take up an equilateral polygonal formation moving on a circle whose center is the target.

In this paper, close target reconnaissance (CTR) using autonomous UAV formations in the presence of obstacles (or no-fly-zones) is considered. To accomplish the aforementioned task of CTR a two-level control scheme is presented. The first level of control moves each agent to a vicinity of the target of interest, and the second level acquires and maintains an equilateral triangular formation of the three UAVs while the UAVs are circling around the target.

This work is supported by NICTA, which is funded by the Australian Government as represented by the Department of Broadband, Communications and the Digital Economy and the Australian Research Council through the ICT Centre of Excellence program.

Iman Shames, Barış Fidan, and Brian D. O. Anderson are with Research School of Information Science and Engineering, Australian National Univeristy and NICTA, ACT 0200, Australia {Iman.Shames, Baris.Fidan, Brian.Anderson}@anu.edu.au

The outline of the paper is as follows. In the next section the cooperative CTR problem is defined and the assumptions made are presented. In Section III a decentralized control scheme is proposed to solve the cooperative CTR problem. In Section IV, some stability analysis is presented of the control laws described in the Section III. Section V presents a set of simulation results. In Section VI a potential extension of the proposed control scheme for 3D space is presented. Some concluding remarks and future problem directions are presented in Section VII.

II. Problem Definition

In this paper we consider the task of CTR of certain targets by a team of three UAVs, each of which is initially located at an arbitrary position. We formally define the overall task of CTR by the following problem definition.

Problem 1 (Close Target Reconnaissance): Three UAVs, namely A_1, A_2, and A_3, have to operate in an environment $\Omega_E \subset \mathbb{R}^2$, containing a stationary target of interest located at $p_g \in \mathbb{R}^2$. Denote the position coordinate vector at time t corresponding to A_i by $p_i(t)$ and assume that each agent knows its current position and the target location, p_g, $\forall t$. The goal is (i) to move A_1, A_2, and A_3 from scattered starting positions, $p_1(0)$, $p_2(0)$, and $p_3(0) \in \Omega_E$, respectively, to the vicinity of p_g and then (ii) form an equilateral triangular formation of A_1, A_2, and A_3 while circling around the target, with side length l and center of mass (CM) at p_g, where l is a predefined constant, i.e. (ii) requires agent position to satisfy $\|p_i - p_g\| = L_g$ and $\|p_i - p_j\| = l$ for each $i, j \in \{1, 2, 3\}$ and $i \neq j$, where $l = \sqrt{3}L_g$.

The overall task formulated in Problem 1 involves individual motion of the UAVs towards the target, avoidance of collision with obstacles and other UAVs, avoidance of entry to no-fly-zones, and once a certain vicinity of the target is reached, forming a triangular formation around the target and maintaining this formation for a certain duration while the agents are rotating around the target. Agents need not reach the vicinity of the target simultaneously. Each of these subtasks or problem subelements is described in detail in subsections II-B and II-C.

A. Agent Models

For each agent A_i, a single integrator point agent model is considered:

$$\dot{p}_i(t) = v_i(t) \tag{1}$$

where $v_i(t)$ is the velocity of the agent, which is used as the control input for each agent. Furthermore, the speeds of the three UAVs are assumed to be constant and equal, which is typical for a fleet of three plane-type UAVs, i.e. $\|v_i(t)\| = \bar{v}$,

$\forall t > 0$, where $\bar{v} > 0$ is a certain constant. This constant speed constraint which is associated with a certain type of UAV, Aerosonde UAV [5], [6], [7], draws a distinction line between the current paper and the other ones that deal with similar problems [3], [4], [8], and [9].

B. Obstacles, No-Fly-Zones, and Inter-Agent Avoidance

Without loss of generality, for each agent A_i we consider physical obstacles, no-fly-zones, and other agents as "obstacles". In addition we assume that each agent A_i detects an obstacle within a range less than or equal to a certain limit r_d, and uses this information to update its own environment map, $\Psi_i(t)$ at time t. In order to define various subregions of each agent's environment map, we first introduce the following notation:

$$\Omega(\overline{x}(t), \overline{y}(t), l, w) = \{(x, y) | \overline{x} \leq x \leq \overline{x} + l, \overline{y} \leq y \leq \overline{y} + w\} \tag{2}$$

denotes the rectangular region on the xy-plane where $(\overline{x}(t), \overline{y}(t)$ are the coordinates of the CM of the rectangular region at time t, l is its length parallel to the x-axis, and w is its width parallel to the y-axis. The overall area of interest is represented by a rectangle,

$$\Omega_E = \Omega(x_0, y_0, L, W). \tag{3}$$

Each agent's own environmental map $\Psi_i(t)$ is a rectangular region with the same size as Ω_E with an overlaid grid structure. A predefined grid resolution value δ_r is assumed, i.e. each of x_0, y_0 , L, and W are assumed to be integer multiples of δ_r. This area of interest defines the boundaries of the environment map of each agent. Furthermore, each obstacle is modeled as a union of rectangular obstacles. The total obstacle region detected by agent A_i at time t is represented by a sequence of M_i rectangles

$$\Omega_{Oij}(t) = \Omega(x_{Oij}(t), y_{Oij}(t), l_{Oij}, w_{Oij}) \tag{4}$$

for $j = 1, \cdots, M_i$, fitting in with the grid structure, i.e. $x_{Oj}(t)$, $y_{Oj}(t)$, l_{Oj}, and w_{Oj} are integer multiples of δ_r for each j. It is assumed that $\Omega_{Oij} \subset \Omega_E$ for each j. Further denote

$$\Omega_{Oi}(t) = \bigcup_{j=1}^{M_i} \Omega_{Oij}(t) \tag{5}$$

In addition $\overline{\Omega}_{Oij}(t)$ is defined as

$$\overline{\Omega}_{Oij}(t) = \Omega(x_{Oij}(t) - \rho, y_{Oij}(t) - \rho, l_{Oij} + 2\rho, w_{Oij} + 2\rho), \quad j = 1, 2, \cdots, M_i \tag{6}$$

in which ρ is a design constant. Furthermore,

$$\overline{\Omega}_{Oi}(t) = \bigcup_{j=1}^{M_i} \overline{\Omega}_{Oij}(t) \tag{7}$$

Assuming that each agent, A_i, knows the locations of any obstacle within Ω_E when its distance from the obstacle is less than r_d, the grid-map generation task, i.e. generation of $\Psi_i(t)$ can be characterized as one the coloring of each of the $(L/\delta_r)(W/\delta_r)$ grid squares of $\Psi_i(t)$, i.e. each,

$$\Omega_g[k, j] = \Omega(x_0 + k\delta_r, y_0 + j\delta_r, \delta_r, \delta_r) \tag{8}$$

where $k \in \{0, 1, \cdots, (L/\delta_r) - 1\}$ and $j \in \{0, 1, \cdots, (W/\delta_r) - 1\}$, with one of three colors: white, black, and gray. For each grid $\Omega_g[k, j]$ the following rule is used for coloring:

1) if $\Omega_g[k, j] \subset \Omega_O$ then color $\Omega_g[k, j]$ black.
2) if $\Omega_g[k, j] \subset \overline{\Omega}_O \setminus \Omega_O$ then color $\Omega_g[k, j]$ gray.
3) Otherwise color $\Omega_g[k, j]$ white.

Remark 1: The agent only detects that part of the obstacle within the detection radius of r_d.

The aim in the above coloring is as follows: The path will pass only through white grid squares, the agents can move through grey and white grid squares,which because of the extended definition of obstacles ensures collision avoidance. This explains the reason for the definition of $\Omega_{Oi}(t)$ and $\overline{\Omega}_{Oi}(t)$. The obstacle avoidance motion algorithm to be used by the agents is based on the above definitions and is described in detail in section III-A.

C. Target Reconnaissance and Formation Acquisition

In order to accomplish the task of CTR the agents should acquire a triangular formation while circling around the target. This requires a control scheme capable of guaranteeing that the agents move to a vicinity of the target and that they establish the desired equilateral triangular formation while they are circling around the target. In Section III-B we discuss the proposed control scheme for this subtask.

III. Proposed Control Scheme

In this section we discuss the decentralized control scheme used to accomplish the CTR task. The control scheme is divided into two control phases. In the first phase, the *motion towards the target phase*, the control laws move each agent to a vicinity of the target while guaranteeing obstacle avoidance (which includes avoidance of inter-agent collision). In the second phase, the *target acquiring phase*, the control laws guarantee inter-agent collision avoidance and establishment of the triangular formation around the target, while the agents circle the target position.

A. Agent Motion Towards the Target

Agents move independently towards the target, taking no account of one another unless for collision avoidance. In order to move towards the goal position each agent A_i maintains its own environment map $\Psi_i(t)$ at time t. Knowing this map, a preliminary path, and a sequence of waypoints (for its use) are computed by the agent, this preliminary environment map is updated locally by each agent when it detects a new obstacle, and after each detection a new waypoint sequence is generated. Then each agent A_i moves towards each waypoint in its generated sequence, one waypoint after another, until it reaches the vicinity of the target, i.e. $\|p_i - p_g\| \leq D$, where $D = 2l + L_g$. In the following subsections the path generation, waypoint generation and the control law which move each agent through the sequence of waypoints are described.

1) Path Planning with A^*: A preliminary path using the A^* algorithm is generated at $t = 0$. The A^* algorithm, is a graph search algorithm that finds a path from a given initial grid square to a given goal grid square. It was introduced by [10], as an effective heuristic improvement of Dijkstra's algorithm, see [11], and it provides a better average performance than Dijkstra's with respect to searched nodes when one only needs the optimum path. The optimality here is defined with respect to traveled distance between two nodes in a directed graph with non-negative weights [12]. We call the path sequence generated by A^* search, S, where S is the set of N points that are centers of adjacent grid squares, with S_i the i-th point of the sequence position vector (the center of i-th grid square). At each time step, $t > 0$ each UAV scans its surrounding environment, to check whether there is a newly detected obstacle or not; if there is, it updates its map of the environment and generates a new path sequence and waypoints. If not, it continues with its previous path sequence. We call an obstacle a detected one when its distance to the agent is less than the detection range, r_d. (Each environmental map,Ψ_i at each time step contains the information about only those obstacles that are currently detected.)

2) Waypoint Generation: After the generation of the path a set of waypoints is generated using an algorithm similar to the one presented in [13] to break the path into smaller parts, by generating some waypoints on the path. We call the sequence of M waypoints as W, and W_i is the i-th waypoint position vector. This algorithm is as follows:

Algorithm 1.

1. $W_1 := S_1$
2. $i := 2;\ j := 1$
3. While $i \leq N$
   a) If the line connecting W_j and S_i is not obstructed by an obstacle then $i := i + 1$ else $j := j + 1$; $W_j = S_{i-1}$
4. End

Hence each agent A_i should visit each of the waypoints in its current waypoint sequence until it reaches a vicinity of the target.

Remark 2: Since for each agent, other agents are considered as obstacles they will not have a path going through those agents, hence collision will not happen. Furthermore each environmental map, Ψ_i at each time step contains the information about only those obstacles that are currently detected, so for example if A_1 is detecting A_2, by any change in the position of A_2, Ψ_1 gets updated.

Remark 3: Agents may get stuck in deadlocks with zero probability, because in a very few number of situations out of infinitely many other situations a deadlock happens. However, one may handle these situation heuristically, e.g. increasing the avoidance region for one of the agents when the cyclic behaviour is taking place.

3) Control Law for Agent Motion Towards the Target: In order to reach a close vicinity of the target and avoiding collision with the obstacles, each agent should move towards waypoints in the order that they occur in its waypoint sequence, W. The following vector controls the motion of i-th agent towards its j-th waypoint, assuming it has already visited its $(j-1)$-th waypoint,

$$v_i(t) = \frac{W_j - p_i(t)}{\|W_j - p_i(t)\|}\bar{v} \qquad j = 1, \cdots, M \tag{9}$$

When the agents enters a ball with W_j as its center and ε_w as its radius it will move to the next waypoint in the waypoint list, W_{j+1}. Of course, it can be that at anytime the waypoint list requires updating due to the detection of new obstacles. When each agent, A_i ($i \in \{1, 2, 3\}$), enters a ball with the goal position, p_g as its center and D as its radius another set of control laws governs their motion. This set of control laws is studied in the next subsection.

B. Reconnaissance in the Close Vicinity of the Target

As mentioned in Problem 1 the objective for the agents is to circle around the target position in an equilateral triangular formation, while keeping their distance from each other.

In what follows control laws for the three agent triangular formation rotating around the goal position are presented. These only apply when the agent is inside the ball $B(p_g, D) = \{x \in \mathbb{R} | \|x - p_g\| \leq D\|$.

It is assumed that each agent obtains an identity as soon as it enters the ball $B(p_g, D)$. The first agent to enter is termed A_1, the second one A_2, and the third one A_3. In this case A_1 we call *leader*, A_2 the *first follower*, and A_3 an *ordinary follower*, using a hierarchical formation structure similar to [7]. Furthermore, we assume that the agents rotate around the target in a counter-clockwise direction. For A_1 we propose the control law,

$$v_1(t) = \frac{v_{p1}(t)}{\|v_{p1}(t)\|}\bar{v} \tag{10}$$

$$v_{p1}(t) = \sigma_1(t)v_{r1}(t) + (1 - |\sigma_1(t)|)v_{t1}(t) \tag{11}$$

where $v_{r1}(t)$ and $v_{t1}(t)$ are, respectively, the radial and tangential components of $v_{p1}(t)$ and $\sigma_1(t) \in [-1, 1]$ is a switching term used to adjust relative ratio of these radial and tangential components for keeping the desired distance from the target, L_g while circling around the target at constant speed. The variables $v_{r1}(t)$, $v_{t1}(t)$, and $\sigma_1(t)$ are all continuous and are defined as follows:

$$\sigma_1(t) = \begin{cases} 1 & d_{g1}(t) > L_g + \varepsilon_g \\ \dfrac{(d_{g1}(t) - L_g)}{\varepsilon_g} & L_g - \varepsilon_g \leq d_{g1}(t) \leq L_g + \varepsilon_g \\ -1 & d_{g1}(t) < L_g - \varepsilon_g \end{cases} \tag{12}$$

$$v_{r1}(t) = \frac{p_g - p_1(t)}{d_{g1}(t)} \tag{13}$$

$$v_{t1}(t) = \begin{bmatrix} 0 & 1 \\ -1 & 0 \end{bmatrix} v_{r1}(t) \tag{14}$$

where $d_{g1}(t) = \|p_g - p_1(t)\|$ and ε_g is the predetermined error tolerance on the agent distance from the target. Let $t_0 = \text{liminf}\{t | \sigma_1(t) \neq 1\}$. At $t = t_0$, A_1 comes to a distance $L_g + \varepsilon_g$ from the target. Assume that for $t \leq t_0$ the tasks

of A_2 and A_3 are only to move towards the goal and form the required formation, i.e. there is no obstacle left to avoid (apart from the other agents) at time t_0. For $t > t_0$ and $p_i \in B(p_g, D)$, the following control laws are proposed govern the motion of A_2 and A_3; For $i = 2, 3$,

$$v_i(t) = \frac{v_{pi}(t)}{\|v_{pi}(t)\|}\bar{v} \tag{15}$$

$$v_{pi} = \sigma_i(t)v_{ai}(t) + (1 - \sigma_i(t))v_{gi}(t) \tag{16}$$

where σ_2, σ_3, v_{ai}, and v_{gi} are defined as follows:

$$\sigma_2(t) \equiv \sigma_2(p_1(t), p_2(t)) = \begin{cases} 1 & d_{12}(t) < l_a - \varepsilon_a \\ \dfrac{(d_{12}(t) - l_a - \varepsilon_a)}{-2\varepsilon_a} & l_a - \varepsilon_a \le d_{12}(t) \le l_a + \varepsilon_a \\ 0 & d_{12}(t) > l_a + \varepsilon_a \end{cases} \tag{17}$$

$$\sigma_3(t) \equiv \sigma_3(p_1(t), p_2(t), p_3(t)) = \begin{cases} 1 & d_3^{min}(t) < l_a - \varepsilon_a \\ \dfrac{(d_3^{min}(t) - l_a - \varepsilon_a)}{-2\varepsilon_a} & l_a - \varepsilon_a \le d_3^{min}(t) \le l_a + \varepsilon_a \\ 0 & d_3^{min}(t) > l_a + \varepsilon_a \end{cases} \tag{18}$$

$$v_{a2}(t) = \frac{p_2(t) - p_1(t)}{d_{12}(t)} \tag{19}$$

$$v_{a3}(t) = \alpha_1 \frac{p_3(t) - p_1(t)}{d_{13}(t)} + \alpha_2 \frac{p_3(t) - p_2(t)}{d_{23}(t)} \tag{20}$$

$$\alpha_i = \begin{cases} 1 & d_{i3}(t) < l_a - \varepsilon_a \\ \dfrac{(d_{i3}(t) - l - \varepsilon_a)}{-2\varepsilon_a} & l_a - \varepsilon_a \le d_{i3}(t) \le l_a + \varepsilon_a \\ 0 & d_{i3}(t) > l_a + \varepsilon_a \end{cases} \tag{21}$$

$i = 2, 3$

$$v_{gi}(t) = \frac{p_{gi}(t) - p_i(t)}{d_{gi}(t)} \quad i = 2, 3 \tag{22}$$

where $d_{12}(t) = \|p_1(t) - p_2(t)\|$, $d_3^{min} = \min\{\|p_1(t) - p_3(t)\|, \|p_3(t) - p_2(t)\|\}$, $d_{i3}(t) = \|p_i(t) - p_3(t)\|$, $d_{gi}(t) = \|p_{gi} - p_i(t)\|$, and $p_{g2}(t)$ and $p_{g3}(t)$ are points on the circle $C(p_g, L_g)$, which can be obtained by moving $p_1(t)$ by $2\pi/3$ and $4\pi/3$ respectively, in clockwise direction on $C(p_g, L_g)$. Furthermore, we choose l_a and ε_a in a way such that, $l_a + \varepsilon_a = l/2$.

Remark 4: One can extend the proposed method for more than three agents by changing the value for angular separation and introducing control laws similar to the third agent here for all the new ones. For instance, the fourth added agent should put itself $\pi/2$ after the third agent.

IV. Analysis of Control Laws

For the control law presented by (9) it is trivial to show that each agent will reach a ball with its next waypoint W_i as its center and a radius of ε_w. For the laws presented in subsection III-A.3, we can state the following.

Theorem 1: Agents A_i, $i \in \{1, 2, 3\}$ starting from points out of the circle $C(p_g, L_g)$ and having initial inter-agent distances larger than l converge to $C(p_g, L_g)$ while their inter-agent distance is equal to l under the control law defined by (10).

Theorem 1 is an immediate corollary of Lemmas 1-3, which are presented next together with proofs or proof sketches. The complete set of proofs will be provided in an extended version of this paper. In the sequel, for the sake of simplicity and without the loss of generality, we assume that $p_g = [0, 0]^T$.

Lemma 1: Agent A_1 controlled by the control law (10)-(14) converge to $C(p_g, L_g)$.

Proof. We define a positive definite function $V_1(p_1(t))$

$$V_1(p_1(t)) = \frac{1}{4}(p_1(t)^T p_1(t) - L_g^2)^2. \tag{23}$$

We have

$$\begin{aligned} \dot{V}_1(p_1(t)) &= p_1(t)^T v_1 (p_1(t)^T p_1(t) - L_g^2) \\ &= p_1(t)^T(\sigma_1(t)v_{r1}(t) + (1 - |\sigma_1(t)|)v_{t1}(t)) \\ &\quad (p_1(t)^T p_1(t) - L_g^2)K_1 \\ &= -\sigma_1(t)\|p_1(t)\|(p_1(t)^T p_1(t) - L_g^2)K_1(t) \end{aligned}$$

where $K_1(t) = \bar{v}/\|v_{p1}(t)\|$ noting that $p_1^T(t)v_{r1}(t) = -\|p_1(t)\|$ and $p_1^T(t)v_{t1} = 0$. Define

$$\Omega^c \triangleq \{x \in \mathbb{R}^2 | \|x\| \le D\}. \tag{24}$$

Here, Ω^c is the points on and inside the circle $C(p_g, D)$. Furthermore, $S_1 \subset \Omega^c$ is

$$S_1 \triangleq \{p_1 \in \Omega^c | \dot{V}_1(p_1) = 0\} \tag{25}$$

It can be easily seen that $S_1 = C(p_g, L_g)$; for $p_1(t) \in \Omega^c \setminus S_1$, $\dot{V}_1(p_1(t)) < 0$, and the largest invariant subset of S_1 is itself. It can be easily seen that the system defined by control law (10)-(14) is actually a time-invariant system, hence we can apply LaSalle's principle [14]. According to LaSalle's principle the trajectory converges to S_1 as $t \to \infty$. □

Lemma 2: Assume that A_1 is moving around the circle $C(p_g, L_g)$ centered at target $p_g = [0, 0]^T$ with constant speed $\bar{v}$ in counterclockwise direction, and consider $p_{g2}(t)$ as defined in Section III. Furthermore assume that, initially (at time $t = 0$) $d_{12}(t) \ge l_a + \varepsilon_a$. Then using the control laws (15)–(17),(19),(22) for agent A_2, the following hold:

(i) $d_{12}(t) \ge l_a - \varepsilon_a$, $\forall\ t \ge 0$.

(ii) $\forall\ t \ge 0$, $\dot{d}_{g2}(t) \le 0$ if $d_{12}(t) \ge l_a + \varepsilon_a$.

(iii) There exist $T, k_{g2} > 0$ such that $d_{g2}(t_0 + T) \le d_{g2}(t_0) - k_{g2}T$ for any time interval $t_0 \le t \le t_0 + T$ for which $\|p_2(t)\| \ge L_g + l_a + \varepsilon_a$. Therefore, there exists a time instant t_g such that $\|p_2(t_g)\| \le L_g + l_a + \varepsilon_a$.

(iv) For any given a positive constant $\bar{\varepsilon}_g$, there exist $T_g, \bar{k}_{g2} > 0$ such that $d_{g2}(t_0 + T_g) \le d_{g2}(t_0) - \bar{k}_{g2}T$ for any time interval $t_0 \le t \le t_0 + T_g$ for which $d_{12}(t) \ge l_a + \varepsilon_a$ and $\|p_2(t)\| \ge L_g + \bar{\varepsilon}_g$.

(v) $p_2(t) \to p_{g2}(t)$, as $t \to \infty$.

Proof Sketch. (i) Consider the positive definite function $V_{12}(t) = \frac{1}{2}e_{12}^T(t)e_{12}(t) = \frac{1}{2}d_{12}^2$, where $e_{12}(t) = p_1(t) - p_2(t)$. We have

$$\begin{aligned}\dot{V}_{12}(t) &= e_{12}^T(t)(\dot{p}_1(t)-\dot{p}_2(t)) \\ &= e_{12}^T(t)(v_1(t)-v_2(t)) \end{aligned} \quad (26)$$

If $d_{12}(t) \leq l_a - \varepsilon_a$, from (17) we have $\sigma_2(t) = 1$ and hence $v_2(t) = v_{a2}(t) = \frac{-\bar{v}}{d_{12}(t)} e_{12}(t)$. Substituting in (26), we obtain

$$\begin{aligned}\dot{V}_{12}(t) &= e_{12}^T(t)v_1(t) + \bar{v}d_{12}(t) \\ &\geq d_{12}(t)(\bar{v} - \|v_1(t)\|) = 0\end{aligned}$$

Therefore, at each time $t \geq 0$ either $\dot{V}_{12}(t) \geq 0$ or $d_{12}(t) > l_a - \varepsilon_a$, which implies that $d_{12}(t) \geq l_a - \varepsilon_a$, $\forall\ t \geq 0$.

(ii) The result follows a procedure similar to that in part (i) using the positive definite function $V_{g2}(t) = \frac{1}{2} e_{g2}^T(t) e_{g2}(t) = \frac{1}{2} d_{g2}^2$ and its time derivative $\dot{V}_{g2}(t) = e_{g2}^T(t)(\dot{p}_{g2}(t) - v_2(t))$, which satisfies

$$\begin{aligned}\dot{V}_{g2}(t) &= e_{g2}^T(t)\dot{p}_{g2}(t) - \bar{v}d_{g2}(t) \\ &\leq d_{g2}(t)(\|\dot{p}_{g2}(t)\| - \bar{v}) = 0\end{aligned} \quad (27)$$

where $e_{g2}(t) = p_{g2}(t) - p_2(t)$, for $d_{12}(t) \geq l_a + \varepsilon_a$. Note here that (27) follows from the dynamics

$$\dot{e}_{g2}(t) = \dot{p}_{g2}(t) - \frac{\bar{v}}{d_{g2}(t)} e_{g2}(t) \quad (28)$$

(iii) (Sketch) The result follows observing that $e_{g2}^T(t)\dot{p}_{g2}(t)/d_{g2}(t)$ regarding (27) varies continuously within the range $[-\bar{v}, \bar{v}]$, when $\|p_2(t)\| \geq L_g + l_a + \varepsilon_a$, $d_{g2}(t_0 + T) \leq d_{g2}(t_0) - k_{g2}T$.

(iv) (Sketch) The reasoning is similar to the one in the proof sketch of (iii).

(v) (Sketch) Treating (28) as a linear time varying system and $-\frac{\bar{v}}{d_{g2}(t)}$ a time varying parameter, the solution to this equation within any time interval $t_0 \leq t \leq t_1$ for which $d_{12}(t) \geq l_a + \varepsilon_a$ is found as

$$\begin{aligned}e_{g2}(t) &= e^{-\bar{v}\int_{t_0}^t d_{g2}^{-1}(s)ds} e_{g2}(t_0) \\ &+ \int_{t_0}^t e^{-\bar{v}\int_\tau^t d_{g2}^{-1}(s)ds} \dot{p}_{g2}(\tau)d\tau\end{aligned} \quad (29)$$

Furthermore, without loss of generality, the time trajectories of p_1,p_{g2},$\dot{p}_1$,$\dot{p}_{g2}$ in global coordinates can be written explicitly as

$$p_1(t) = L_g\varphi\left(\frac{\bar{v}t}{L_g}\right) \quad (30)$$

$$p_{g2}(t) = L_g\varphi\left(\frac{\bar{v}t}{L_g} - \frac{2\pi}{3}\right) \quad (31)$$

$$\dot{p}_1(t) = \bar{v}\varphi\left(\frac{\bar{v}t}{L_g} + \frac{\pi}{2}\right) \quad (32)$$

$$\dot{p}_{g2}(t) = \bar{v}\varphi\left(\frac{\bar{v}t}{L_g} - \frac{\pi}{6}\right) \quad (33)$$

where $\varphi(\theta) \triangleq [\cos\theta,\ \sin\theta]^T$ for any $\theta \in \mathbb{R}$.

The procedure to be followed in the extended version of this paper to establish (v) is to be based on further exploitation of (29) together with (33) as well as the results (i)–(iv). □

Lemma 3: Assume that A_1 and A_2 are moving around the circle $C(p_g, L_g)$ centered at target $p_g = [0,0]^T$ with constant speed $\bar{v}$ in counterclockwise direction, the corresponding positions $p_1(t)$, $p_2(t) = p_{g2}(t)$ being given by (30),(31). Consider $p_{g3}(t) \triangleq L_g\varphi\left(\frac{\bar{v}t}{L_g} + \frac{2\pi}{3}\right)$. Furthermore assume that, initially (at time $t = 0$) $d_{13}(t), d_{23}(t) \geq l_a + \varepsilon_a$. Then using the control laws (15), (16),(18),(20)–(22) for agent A_3, the following hold:

(i) $d_{13}(t), d_{23}(t) \geq l_a - \varepsilon_a$, $\forall\ t \geq 0$.

(ii) $\forall\ t \geq 0$, $\dot{d}_{g3}(t) \leq 0$ if $d_3^{min}(t) \geq l_a + \varepsilon_a$.

(iii) There exists $T, k_{g3} > 0$ such that $d_{g3}(t_0 + T) \leq d_{g3}(t_0) - k_{g3}T$ for any time interval $t_0 \leq t \leq t_0 + T$ for which $\|p_3(t)\| \geq L_g + l_a + \varepsilon_a$. Therefore, there exists a time instant t_g such that $\|p_3(t_g)\| \leq L_g + l_a + \varepsilon_a$.

(iv) For any given a positive constant $\bar{\varepsilon}_g$, There exist $T_g, \bar{k}_{g3} > 0$ such that $d_{g3}(t_0 + T_g) \leq d_{g3}(t_0) - \bar{k}_{g3}T$ for any time interval $t_0 \leq t \leq t_0 + T_g$ for which $d_3^{min}(t) \geq l_a + \varepsilon_a$ and $\|p_3(t)\| \geq L_g + \bar{\varepsilon}_g$.

(v) $p_3(t) \to p_{g3}(t)$, as $t \to \infty$.

Proof Sketch. The proof sketch is similar to that of Lemma 2 and omitted. □

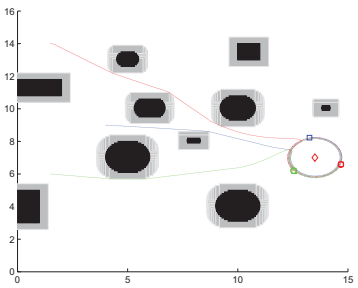

Fig. 1. The agents starting from scattered positions construct an equilateral triangular formation around the target without colliding with any of the obstacles or each other. The blue line is the trajectory of A_1, green is the trajectory of A_2 and red is the trajectory of A_3.

V. Simulations

In this section some simulation results are presented to show how the control laws presented in Section III perform. In the first simulation the agents controlled by the control laws presented in subsections III-A and III-B are tested in an environment Ω_E in the presence of the obstacles. Fig. 1 shows the result of this simulation. In the second simulation an environment with different obstacles, different starting positions for the agents and the goal position is considered. Fig. 2 show the result of these simulations.

VI. Extension of The Control Scheme for 3D

In this section we consider the situation when the agents' starting positions lies in different z-planes , i.e. they have different starting altitudes. The agents maintain their altitude until they enter a vertical cylinder of radius D with axis through p_g. As for the 2D case, the path planning and moving through the waypoints is as described in subsection III-A in each agent's plane. When each agent enters the cylinder described above, the following control law governs the agents for constructing a triangular formation around the target in an agreed plane perpendicular to z axis, i.e. $z = z_d$ plane.

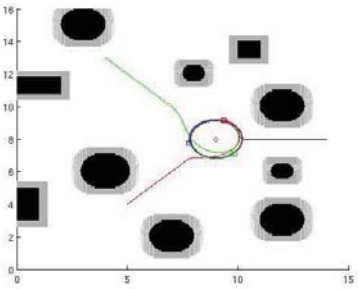

Fig. 2. The agents starting from scattered positions construct an equilateral triangular formation around the target without colliding with any of the obstacles or each other. The blue line is the trajectory of A_1, red is the trajectory of A_2 and green is the trajectory of A_3.

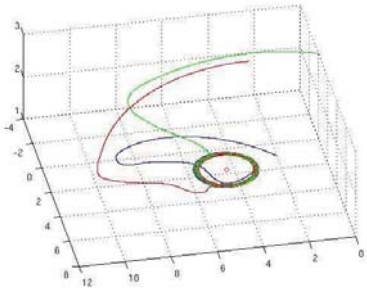

Fig. 3. The agents starting from different positions in in $\mathbb{R}^3$ move to an agreed plane and construct an equilateral triangular formation.

It interposes as a second stage a descend/ascend component prior to assembly around the target.

$$v_i(t) = v_{ni}(t)\bar{v} \tag{34}$$

$$v_{ni}(t) = (v_{ni,x}(t), \quad v_{ni,y}(t), \quad v_{ni,z}(t)) \tag{35}$$

$$v_{ni,x}(t) = \sqrt{\frac{1-\alpha_z^2}{1+(v_{mi,y}(t)/v_{mi,x}(t))^2}}.\text{sgn}(v_{mi,x}(t)) \tag{36}$$

$$v_{ni,y}(t) = |v_{ni,x}(t)|.|v_{mi,y}(t)|/|v_{mi,x}(t)|.\text{sgn}(v_{mi,y}(t)) \tag{37}$$

$$v_{ni,z}(t) = \alpha_z(t).\text{sgn}(v_{mi,z}(t)) \tag{38}$$

$$v_{mi}(t) = \tilde{v}_{mi}(t)/\|\tilde{v}_{mi}(t)\| \tag{39}$$

$$\tilde{v}_{mi}(t) = \sigma_{zi}(t)v_{zi}(t) + (1-\sigma_{zi}(t))v_{pi}(t) \tag{40}$$

$$\sigma_{zi}(t) = \begin{cases} 1 & \|z_d - p_{i,z}(t)\| > \varepsilon_z \\ \dfrac{\|z_d - p_{i,z}(t)\|}{\varepsilon_z} & \|z_d - p_{i,z}(t)\| \leq \varepsilon_z \end{cases} \tag{41}$$

$$v_{zi}(t) = (v_{ti,x}(t), v_{ti,y}(t), \alpha_z \frac{z_d - p_{i,z}(t)}{\|z_d - p_{i,z}(t)\|}) \tag{42}$$

$$v_{ti,x}(t) = v_{ri,y}(t) \tag{43}$$

$$v_{ti,y}(t) = -v_{ri,x}(t) \tag{44}$$

$$v_{ri}(t) = \frac{p_g - p_i(t)}{\|p_g - p_i(t)\|} \tag{45}$$

$$\alpha_z = \frac{\bar{v}_z}{\bar{v}} \tag{46}$$

where $\bar{v}_z$ is the ascend and descend speed of each agent,and $v_{mi,x}(t)$ and $v_{mi,y}(t)$ are x and y components of v_{mi} respectively. A simulation result for 3D case is presented in Fig. 3.

VII. Concluding Remarks and Future Directions

In this paper the problem of CTR by a formation of 3 UAVs is addressed and a control law is presented for the two dimensional case that all the agents remain in same plane. In addition, the convergence of the agents to a desired equilateral triangular formation under the control laws based on unidirectional sensing and distance keeping is analyzed. It should be noted that the control law can be applied to cooperative surveillance tasks involving more than three UAVs with only minor modifications, e.g. changing interagent angular separations in the last part of the control law. An extension to three dimension has been presented as well.

Possible future works and directions include consideration of more practical UAV models and introduction of algorithms with less need for computational resources.

References

[1] Dixon, S.R., Wickens, C.D.: Control of multiple uavs-a workload analysis. In: Proceedings 12th International Symposium Aviation Psychology, Dayton, Ohio (2003)

[2] Finn, A., Kabacinski, K., Drake, S.P.: Design challenges for an autonomous cooperative of uavs. In: Proceedings Information, Decision and Control, Adelaide, Australia (2007)

[3] Marshall, J.A., Broucke, M.E., Francis, B.A.: Formations of vehicles in cyclic pursuit. IEEE Transactions on Automatic Control **49** (2004) 1963–1974

[4] Marshall, J.A., Broucke, M.E., Francis, B.A.: Pursuit formations of unicycles. Automatica **42** (2006) 3–12

[5] http://www.aerosonde.com.

[6] van der Walle, D., Fidan, B., Sutton, A., Yu, C., Anderson, B.: Non-hierarchical uav formation control for surveillance tasks. (In: Proceedings of American Control Conference) 777–782

[7] Sutton, A., Fidan, B., van der Walle, D.: Hierarchical uav formation control for cooperative surveillance. In: Proc. 17th World Congress of Int. Federation of Automatic Control (IFAC'08), Seoul, Korea (2008)

[8] Kim, T.H., Sugie, T.: Cooperative control for target-capturing task based on a cyclic pursuit strategy. Automatica **43** (2007) 1426–1431

[9] Sinha, A., Ghose, D.: Generalization of the cyclic pursuit problem. In: Proceedings of American Control Conference, Portland, OR (2005)

[10] Nilsson, N.J.: Principles of Artificial Intelligence. Springer-Verlag, Berlin (1982)

[11] Dijkstra, E.W.: A note on two problems in connexion with graphs. Numerische Mathematik **1** (1959) 269 –271

[12] Hao, Y., Agrawal, S.K.: Planning and control of ugv formations in a dynamic environment: A practical framework with experiments. Robotics and Autonomous Systems **51** (2005) 101–110

[13] Shames, I., Yu, C., Fidan, B., Anderson, B.D.O.: Externally excited coordination of autonomous formations. In: Proceeding of Mediterranean Conference on Control and Automation, Athens, Greece (2007)

[14] Sastry, S.: Nonlinear Systems: Analysis, Stability, and Control. Springer-Verlag, Berlin (1999)